ORNL/TM-2016/456

Oak Ridge National Laboratory 2nd Generation ODS FeCrAl Alloy Development For Accident-Tolerant Fuel Cladding

Approved for public release.
Distribution is unlimited.

Sebastien Dryepondt
Caleb Massey
Philip. D. Edmondson

August 26, 2016

OAK RIDGE NATIONAL LABORATORY
MANAGED BY UT-BATTELLE FOR THE US DEPARTMENT OF ENERGY

ORNL/TM-2016/456

FCRD Advanced Fuels Campaign

2nd Generation FeCrAl ODS Alloy Development For Accident-Tolerant Fuel Cladding

Sebastien Dryepondt
Caleb Massey
Philip D. Edmonson

Date Published:

August 2016

Prepared by
OAK RIDGE NATIONAL LABORATORY
Oak Ridge, Tennessee 37831-6283

managed by
UT-BATTELLE, LLC
for the
US DEPARTMENT OF ENERGY
under contract DE-AC05-00OR22725

CONTENTS

Page

LIST OF FIGURES

Figure **Page**

LIST OF TABLES

Table **Page**

EXECUTIVE SUMMARY

Extensive research at ORNL aims at developing advanced low-Cr high strength FeCrAl alloys for accident tolerant fuel cladding. One task focuses on the fabrication of new low-Cr oxide dispersion strengthened (ODS) FeCrAl alloys. The first Fe-12Cr-5Al+Y_2O_3 (+ ZrO_2 or TiO_2) ODS alloys exhibited excellent tensile strength up to 800ºC and good oxidation resistance in steam up to 1400ºC, but very limited plastic deformation at temperatures from 25 to 800ºC. To improve alloy ductility, several fabrication parameters were considered. New Fe-10-12Cr-6Al gas-atomized powders containing 0.15 to 0.5wt% Zr were procured and ball milled for 10h, 20h or 40h with Y_2O_3. The resulting powder was then extruded at temperatures ranging from 900 to 1050ºC. Decreasing the ball milling time or increasing the extrusion temperature changed the alloy grain size leading to lower strength but enhanced ductility. Small variations of the Cr, Zr, O and N content did not seem to significantly impact the alloy tensile properties, and, overall, these new 2nd generation ODS FeCrAl alloys showed significantly better ductility than the 1st generation alloys. Tube fabrication needed for fuel cladding will require cold or warm working associated with softening heat treatments. Therefore, work was initiated to assess the effect of these fabrications steps on the alloy microstructure and properties.

This report has been submitted as fulfillment of milestone M3FT-16OR020202091 titled, “Report on 2nd Generation FeCrAl ODS Alloy Development” for the Department of Energy Office of Nuclear Energy, Advanced Fuel Campaign of the Fuel Cycle R&D program.

1. INTRODUCTION

The Fukushima Daiichi accident has led to a renewed interest in advanced materials for accident tolerant fuel cladding. [1,2] One key requirement is good oxidation resistance in steam at high temperature, and extensive work at ORNL has been conducted to develop new low-Cr high strength oxidation resistant FeCrAl alloys. [3-6] Lowering the Cr level hinders the formation of the embrittling Cr-rich α' phase under irradiation,[7] and the higher strength at low temperature allows for the use of thinner cladding, thus limiting the neutronic penalty from the replacement of Zr-based alloys by Fe-based alloys.[8]

To further increase the FeCrAl alloy strength, one of the project tasks aimed at developing new low-Cr oxide dispersion strengthened (ODS) FeCrAl alloys. Fe-12Cr-5Al gas atomized powder was ball milled for 40h with Y_2O_3, Y_2O_3+FeO, Y_2O_3+ZrO_2 (125YZ alloy) and Y_2O_3+TiO_2 to fabricate Fe-12Cr-5Al ODS alloys with various minor additions. [9-11] A very small grain microstructure was observed, in the 100-500 nm size, with grain aspect ratio lower than 2. Transmission electron microscopy revealed the presence of (Al,Y)-rich nano oxides and Zr-rich carbonitrides for alloy 125YZ,[12] but no Zr-rich oxides, as observed by Dou et al.[13]

All the alloys except the one containing Ti exhibited excellent oxidation resistance in steam up to 1450ºC and very good tensile strength up to 800ºC. [9-11] The ductility of these alloys was however quite low at T<400ºC, typically less than 10% plastic deformation at rupture, and this project focused in FY16 on the improvement of the ODS FeCrAl alloy ductility. One concern was the excessive oxygen content in ODS alloys fabricated by ball milling with a combination of two oxides such as Y_2O_3 and ZrO_2, so new gas atomized powders were purchased, with additions of Zr or Zr and Ti. To assess the effect of Zr content on the alloy microstructure and properties, the Zr concentration in the powders was varied from 0.15wt% to 0.5wt%. Controlling the impurity content may also improve the alloy ductility. Ball milling duration was therefore reduced from 40h to 20h and 10h to reduce the C and N pick up during this fabrication step. Finally, the impact of the extrusion temperature on the alloys microstructure and properties was investigated.[15]

2. EXPERIMENTAL PROCEDURE

2.1 Materials

Fe-12Cr-5Al, Fe-12Cr-5.6Al-0.5Zr, Fe-12Cr-5.6Al-0.25Zr-0.13Ti, Fe-10Cr-6.1Al-0.3Zr, Fe-10Cr-6.1Al-0.15Zr and Fe-10Cr-6.1Al gas atomized powders were purchased from ATI Metals powders with a powder size ranging from 45 to 150µm (-100/325 mesh size). The powder compositions are summarized in Table 1. A Zoz CM08 Simoloyer was used to fabricate the 1st generation 125YZ alloy by ball milling for 40h the Fe-12Cr-5Al powder with $Y_2O3+ZrO_2$ powder in Ar atmosphere. The powder was then degassed in a 4 inch cylindrical extrusion can at 300ºC for 24h, and extruded at 950ºC through a rectangular 2 inch x1.5 inch die. The Zoz CM08 Simoloyer was also utilized to fabricate the 2nd generation 126ZY alloy by ball milling together Fe-12Cr-5.6Al-0.5Zr and Y_2O_3 powders. All the other 2nd generation ODS FeCrAl alloys were fabricated using a smaller Zoz CM01. The Fe-10Cr-6.1Al-0.3Zr powder was ball milled for 10h, 20h and 40h with Y_2O_3 powder in Ar atmosphere, but all the other powders were ball milled for 40h only. The powders were then sealed in 2 inch cans, degassed at 300ºC for 24h, and extruded at temperature ranging from 900 to 1050ºC though a 7/8" cylindrical die. The fabrication parameters and alloy composition are summarized in Table 2. Contamination from previous ball milling runs led to a significant amount of Zr in the alloy fabricated from the Fe-10Cr-6.1Al powder. The C content was kept below 200ppm for all of the alloys except for the 1st generation 125YZ and alloy 126ZTY-10C. More variation from one alloy to another was observed for the O and N concentration.

Table 1: Composition in weight % of the gas atomized powders measured by ATI Metal Powder and composition of some ball milled powders measured by ICP spectroscopy, combustion and IGF analysis

		Fe	Cr	Al	Zr	Y	C (ppm)	N (ppm)	O (ppm)	S (ppm)	Other
Gas Atomized	12Cr-5Al	82.8	12.1	5			31	10	64	<3	0.004Si
	12Cr-5.6Al-0.5Zr	81.8	11.9	5.6	0.54		20	20	140	20	0.01Si
	12Cr-5.6Al-0.25Zr-0.13Ti	81.3	12.2	5.9	0.24		40	20	130	30	0.14Ti-0.01Si
	10Cr-6.1Al-0.3Zr	83.1	10	6.4	0.29		40	20	190	30	
	10Cr-6.1Al-0.15Zr	83.1	10.2	6.3	0.15		40	20	190	20	0.01Si
	10Cr-6.1Al	83.7	10	6.1			20	30	190	20	0.01Si
Ball Milled	12Cr-5.6Al-0.5Z-Y 40h	81.06	11.97	5.52	0.49	0.19	190	133	1360	50	0.22Ni-0.14Mn
	106ZY 40h	81.08	9.95	5.98	0.3	0.2	250	610	1490	40	0.04Co-0.03Si
	106ZY 10h	83.07	10.05	6.13	0.3	0.2	70	127	1320	20	0.03Co

Table 2: Fabrication parameters and alloys composition in weight % measured by ICP spectroscopy, combustion and IGF analysis

Alloy Designation	Extrusion Temperature (°C)	Ball Milling Time (h)	Fe	Cr	Al	Zr	Y	C (ppm)	N (ppm)	O (ppm)	S (ppm)
125YZ (1rst gen)	950	40 (CM08)	82.8	11.51	4.86	0.3	0.19	250	161	1920	10
126ZY-10C	1000	40 (CM08)	81.59	11.54	5.61	0.4	0.2	150	103	1110	30
126ZTY-10C	1000	40	82.44	11.26	5.4	0.22Zr-0.12Ti	0.21	330	246	1840	30
106Z(.15)Y-10C	1000	40	83.73	9.64	5.96	0.14	0.18	180	840	1580	30
106Z(.20)Y-10C	1000	40	83.63	9.57	6.01	0.21	0.22	190	226	2220	40
106ZY-10C	1000	40	83.41	9.74	6.02	0.28	0.22	190	580	1290	30
106ZY-9C	900	40	83.34	9.73	6.07	0.28	0.21	170	919	1300	30
106ZY-15C	1050	40	83.69	9.59	5.89	0.27	0.2	170	668	1890	30
106ZY_40h	950	40	83.39	9.68	6.1	0.28	0.21	180	564	1400	30
106ZY_20h	950	20	83.33	9.82	6.14	0.29	0.21	100	181	1080	50
106ZY_10h	950	10	83.29	9.83	6.17	0.28	0.21	50	146	1160	50

2.2 Tensile testing

Sub-sized tensile specimens (SS-3) with a 7.62 mm long and 0.762 or 1mm thick gage section were machined along the alloy extrusion direction. Tensile testing was carried out at 20-800ºC with a strain rate of $10^{-3}s^{-1}$ using an Instron electro-mechanical machine.

2.3 Oxidation testing

Rectangular ~20x10x1-1.5mm coupons were polished to a 600 grit surface finish and then cleaned in acetone and methanol. Isothermal oxidation experiments were conducted at 1200ºC in 100% steam using a magnetic suspension Rubotherm DynTHERM thermogravimetric analyzer (TGA). A high temperature steam furnace was used to conduct oxidation testing at 1400ºC in air or steam. The specimens were heated up with a constant heating rate in 1.5h-3h to 1400ºC in an Ar environment and then exposed to steam flowing at a rate of 200ml/h for 4h.

2.4 Microstructure characterization

As extruded and oxidized coupons were mounted and polished using standard metallographic techniques. The microstructure of the alloy and/or the oxide scale was then characterized using a JEOL model 6500 Field Emission Gun Scanning Electron Microscope (FEG-SEM). The transmission electron microscopy (TEM) specimens were extracted by Focused Ion Beam (FIB, Hitachi model NB500) using the in-situ lift-out method. TEM microstructure analysis was conducted using an FEI Talos F200X (S/TEM).

3. RESULTS

3.1 Effect of ball milling time

As can be seen in Table 1 and Table 2 reducing the ball milling time leads to a significant decrease of the C and N concentration in the ball milled powder and extruded ODS FeCrAl alloy. The tensile properties of the 2nd generation 106ZY alloys ball milled for 10h, 20h and 40h are compared in Figure 1 with the properties of the 1st generation ODS 125YZ alloy and a high strength wrought FeCrAlY alloy developed at ORNL.[6] Increasing the ball milling time led to an increase of the alloy strength and a decrease of the alloy ductility. The ultimate tensile strength (UTS) of these alloys lie between the UTS of the 125YZ alloy and the FeCrAlY alloy. A significant improvement of the ductility was observed for the three 106ZY alloys at all temperatures in comparison with the 125YZ alloy. Figure 2 compares SEM images of the 106ZY-10h, 106ZY-20h and 106ZY -40h alloys with an SEM micrograph the 125YZ alloy. A bi-modal grain distribution was observed for the 106ZY-10h and 106ZY-20h alloys, with larger grains more frequent for the 106ZY-10h alloy. The 106ZY-40h was more homogeneous with a smaller grain size, but still larger than the 125YZ grain size. The three 106ZY alloys also exhibited a larger grain aspect ratio in comparison with the 125YZ alloy. The bimodal grain distribution is the likely explanation for the lower strength of the 106ZY-10h and 106ZY-20h alloys in comparison with the 106ZY-40h alloy. The better alloy ductility is either due to the bimodal grain distribution or the significant decrease of the C and N concentration due to the decrease of the ball milling time (Table 1 and Table 2).

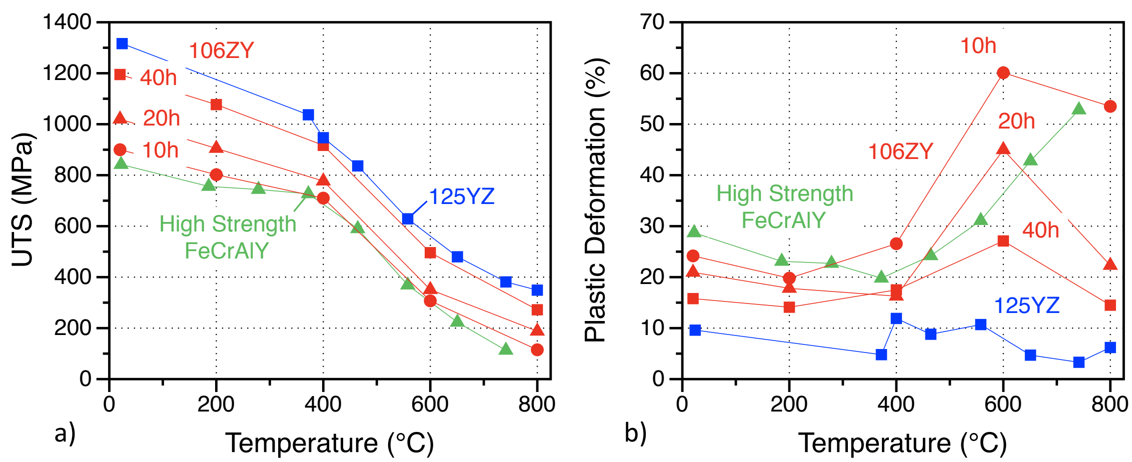

Figure 1: Comparison of the tensile properties of 2nd generation 106ZY alloys fabricated with powders ball milled for 10h, 20h and 40h with 1^{rst} generation ODS 125YZ alloy and a high strength FeCrAl alloy developed at ORNL[6], a) Ultimate tensile strength (UTS), b) Plastic deformation

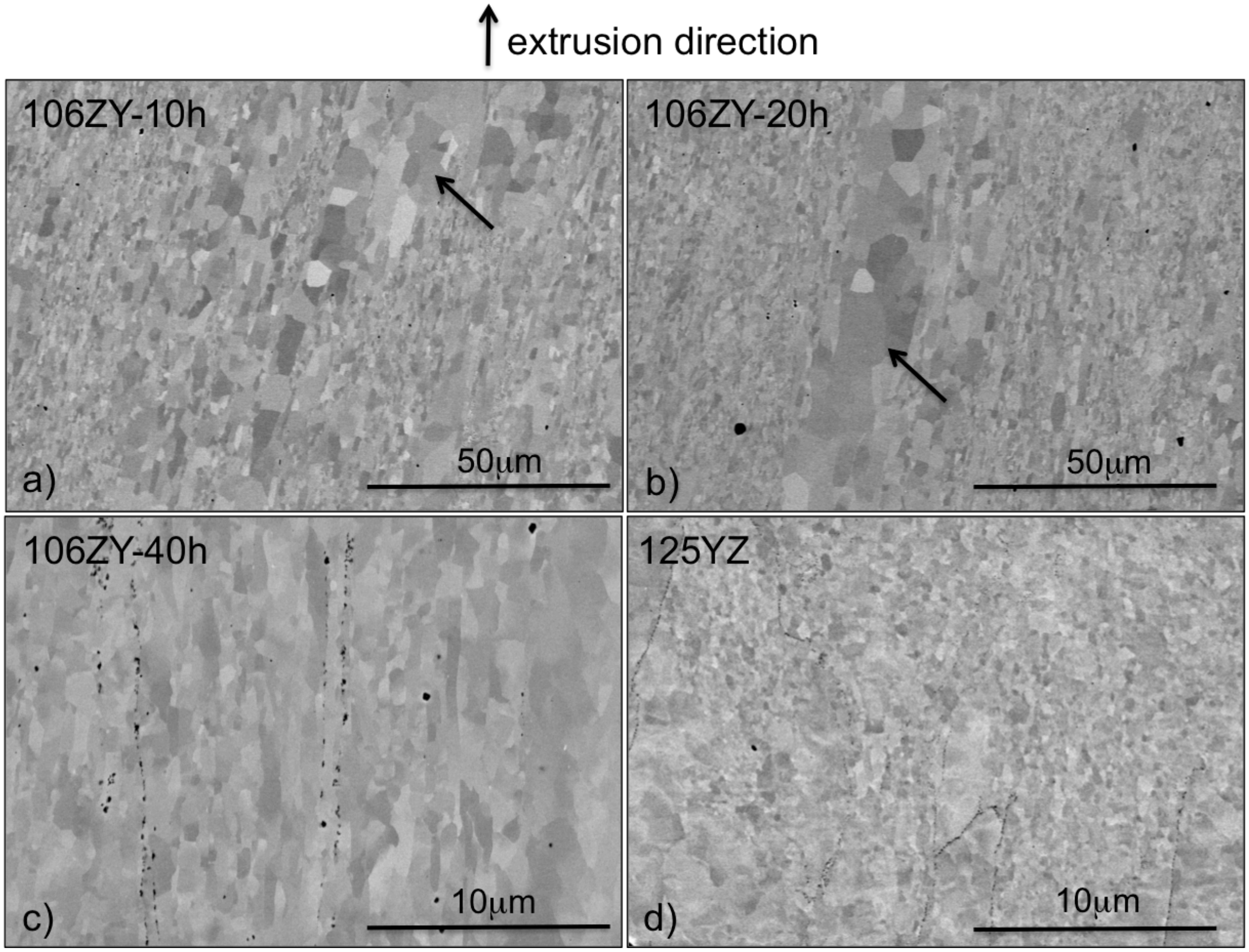

Figure 2: Back scattered (BS) SEM images showing the grain structure of alloy a) 106ZY-10h, b) 106ZY-20h, c) 106ZY-40h and d) 125YZ. Scale bars for a) and b) are five times larger than scale bars for c) and d). Black arrows highlight large grain areas

3.2 Effect of extrusion temperature

The tensile properties of the 106ZY alloys extruded at temperature ranging from 900ºC to1050ºC are compared in Figure 3 with the properties of the 1st generation alloy 125YZ. For the 106ZY alloys extruded at 950, 1000 and 1050ºC, increasing the extrusion temperature led to a decrease of the alloy strength at temperature below ~600ºC. At 800ºC, the three alloys exhibited similar UTS values. The plastic deformations of these three alloys were also quite close, and again significantly better than the plastic deformation of alloy 125YZ. A typical peak of ductility for ODS FeCrAl alloys was observed at ~600ºC. [9] The alloy extruded at 900ºC exhibited slightly higher strength than the 125YZ alloy at all temperatures, and the alloy ductility was slightly inferior to the ductility of the alloys extruded at higher temperatures, but still superior to the ductility of the 125YZ alloy. The microstructure of the 106ZY alloys extruded at 1050ºC, 1000ºC and 900ºC are shown in Figure 4, and can be compared with the microstructure of the alloy extruded at 950ºC and the 125YZ alloy in Figure 2c and 2d.

Increasing the extrusion temperature from 900 to 1050ºC resulted in a small increase of the grain size, but the microstructure remained homogeneous. It is worth noting that the grain size of the high strength 106ZY-9C alloy was still larger than the grain size of the 125YZ alloy. In addition, clusters of small precipitates, most likely Al nitrides due to the high Al content in the 106ZY-9C alloy (Table 2), were observed locally in this alloy (Figure 4d). TEM characterization was initiated and micrographs are shown in Figure 5 and Figure 6 for alloys 106ZY-40h and 106ZY-9C, respectively. Multivariate statistical analysis revealed the presence of small Zr-rich carbonitrides in both alloys, consistent with what was previously observed with alloy 125YZ. Larger alumina particles and Y segregation at some grain boundaries also were observed. Further analysis is required to determine the presence of smaller (Y,Al)-rich oxides detected in alloy 125YZ. [11]

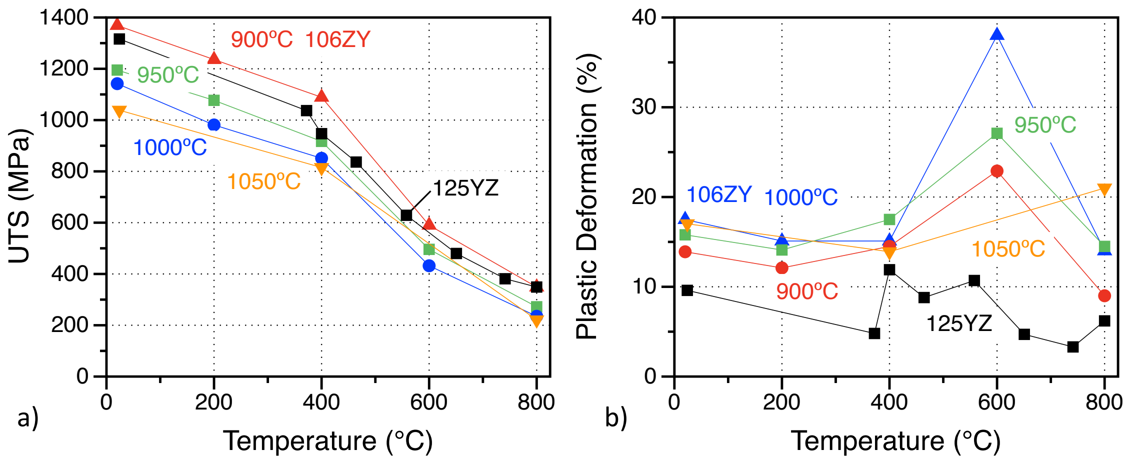

Figure 3: Tensile properties of alloy 125YZ extruded at 950ºC and alloy 106ZY extruded at 900-1050ºC, a) Ultimate tensile stress and b) Plastic deformation

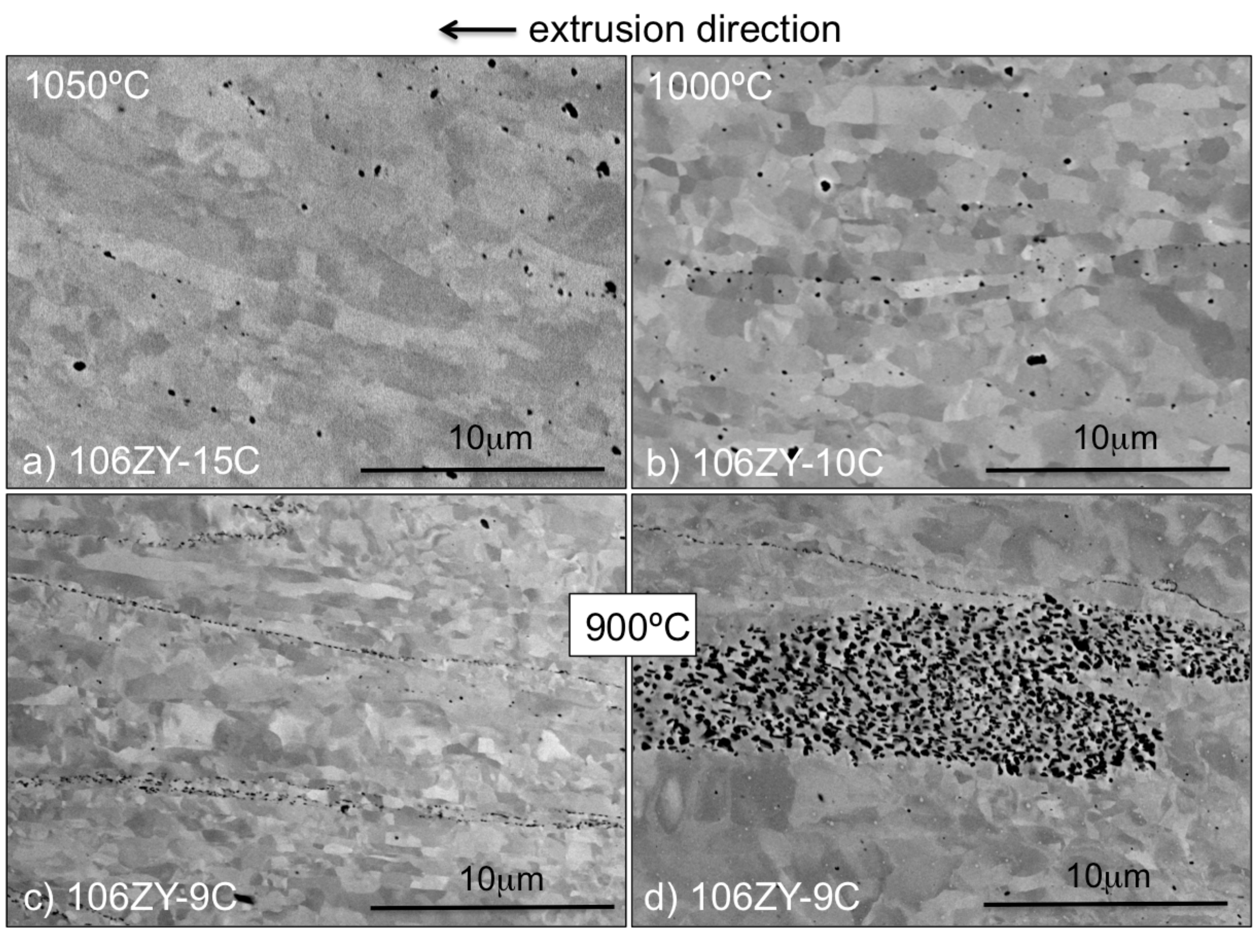

Figure 4: BSE-SEM micrographs showing the grain structure of 106ZY alloys extruded at a) 1050ºC, b) 1000ºC, c) 900ºC and d) 900ºC local cluster of small precipitates

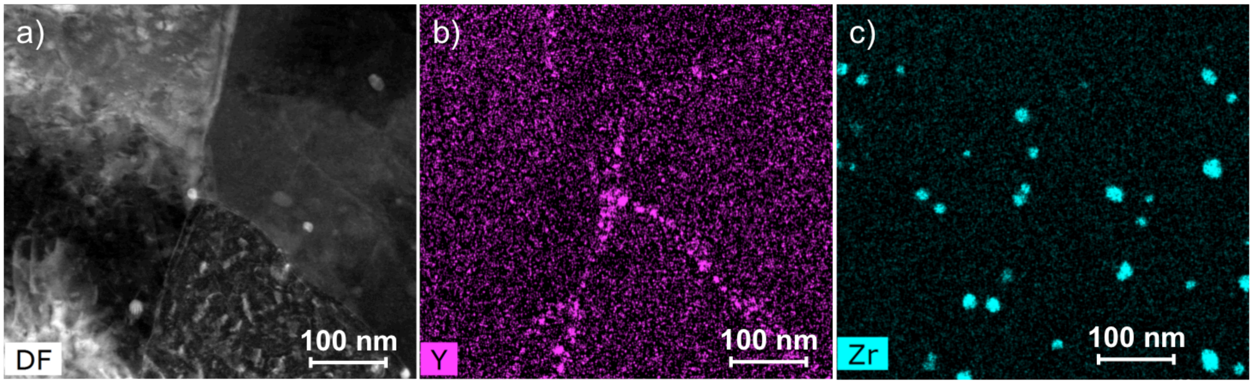

Figure 5: TEM micrographs of alloy 106ZY-40h showing segregation of Y at the alloy grain boundary and the formation of small Zr-rich particles

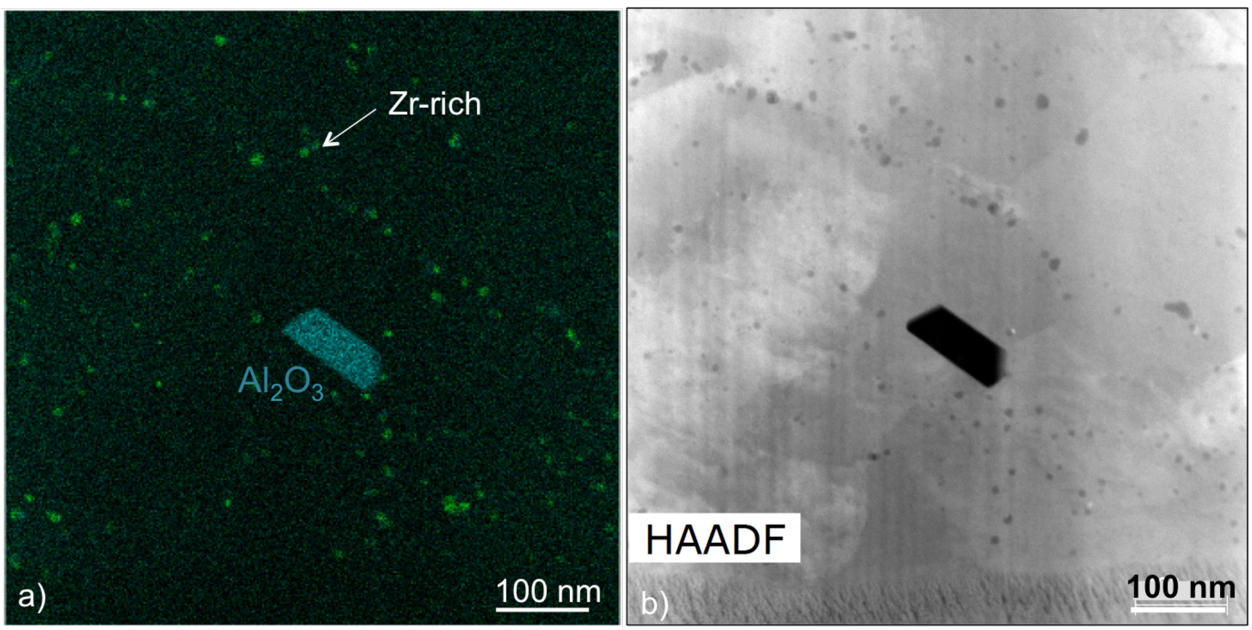

Figure 6: TEM micrographs of alloy 106ZY-9C showing small Zr-rich particles and a larger alumina precipitate

3.3 Chemical composition effect

The tensile properties of the of the 106Z(15)Y, 106Z(20)Y, 106ZY-40h (0.3Zr) 126ZY and 126ZTY alloys are compared in Figure 7. The tensile properties of the 126ZY and 126ZTY alloys were very similar at all temperatures, and slightly higher at T<600ºC than the tensile strength of the 10Cr-6Al alloys. The UTS values at 800ºC were very close for all the alloys, slightly above 200MPa. SEM characterization of these alloys was initiated and some micrographs are shown in Figure 8. The grain structure looks similar for the 126ZY, 126ZTY, 106Z(.15)Y and 106Z(.20)Y alloys, with a higher fraction of Al-rich particles in the 106Z(.15)Y alloy, which could be due to the higher N content in the alloy (Table 2).

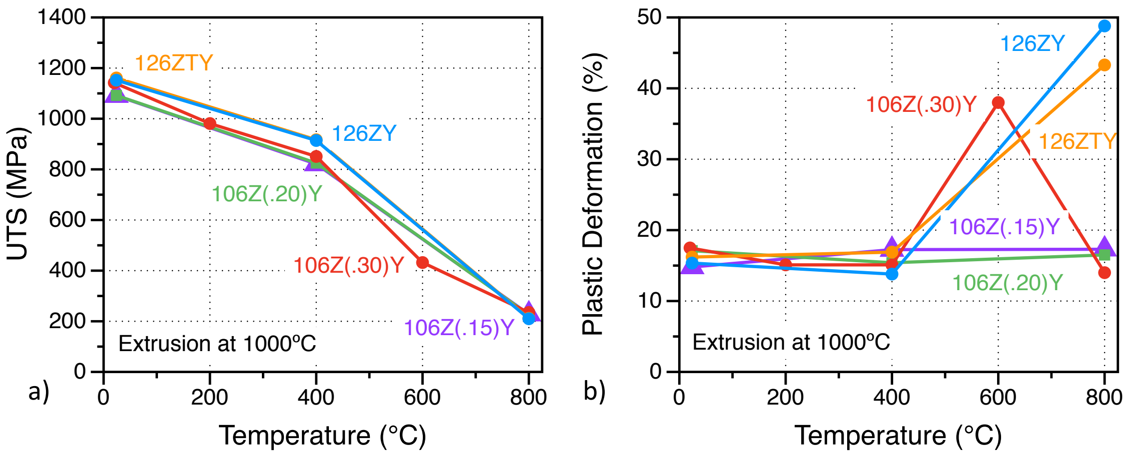

Figure 7: Tensile properties of 106Z(.15)Y, 106Z(.20)Y, 106Z(.30)Y (also named 106ZY-40h), 126ZY and 126ZTY alloys extruded at 1000ºC, a) UTS and b) Plastic deformation

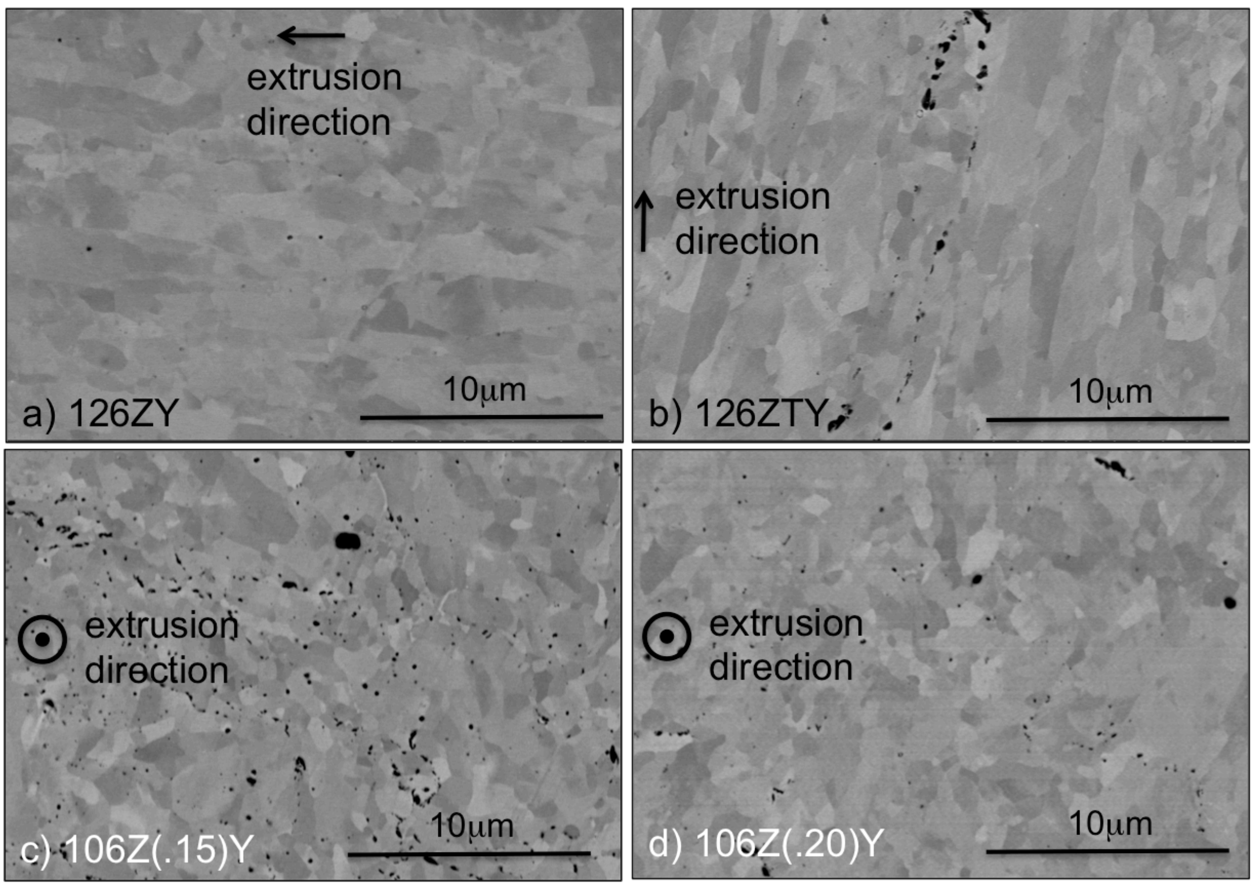

Figure 8: BSE-SEM micrographs showing the grain structure of alloys extruded at 1000ºC, a) 126ZY, b) 126ZTY, c) 106Z(.15)Y and d) 106Z(0.2)Y

3.4 Oxidation Testing

Oxidation testing of alloy 106ZY-40h and 106ZY-9C at 1200ºC for 4h in steam resulted in low mass gain consistent with the growth of a protective alumina scale. As can be seen in the SEM cross section micrographs presented in Figure 9a and 9b, the oxide scale grown at the surface of alloy 106ZT-40h was slightly thinner than the scale observed on alloy 125YZ tested under similar conditions. Zr-rich oxide grains were observed at the scale surface and, locally, in the alumina scale. The 106ZY-40h, 106ZY-9C, 106ZY-10C and 106ZY-10h alloys were oxidized at 1400ºC for 4h in steam and all the coupons failed, with massive mass gains due to the formation of Fe-rich oxides. 106ZY-40h, 106ZY-10C and 106Z-20h specimens were then tested at 1400ºC in air, and again all the specimens except one 106ZY-40h coupon were completely oxidized after 4h. The cross section SEM image of this 106ZY-40h coupon (Figure 9c) shows, however, a thick and porous scale with small areas where the scale was thin and protective (white arrow). A similar scale was observed locally at the surface of the 1st generation 125YF alloy after 4h at 1400ºC in steam.[10] As can be seen in Figure 10, the oxide scale remains an alumina scale with small Zr precipitates. As was observed with the 1st generation ODS FeCrAl,[10] the loss of protectiveness at very high temperature for the 2nd generation ODS FeCrAl is due to a destabilization of the alumina scale, likely because of the significant deformation of the scale/substrate interface during oxidation at high temperature. Further characterization of the alloy microstructure stability at very high temperature is required to understand the lower oxidation performance of the 2nd generation ODS alloys in comparison with the 1st generation ODS alloys.

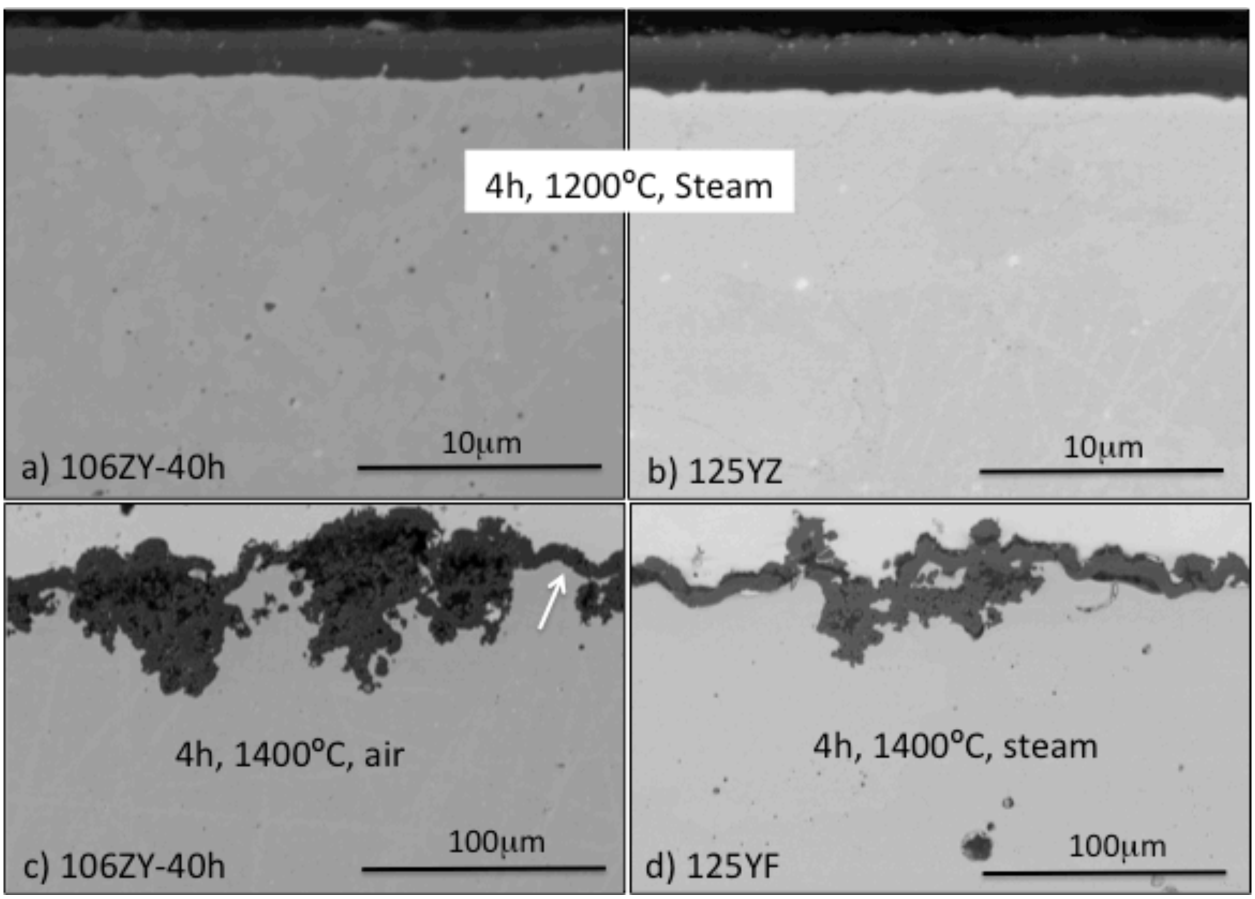

Figure 9: BSE-SEM micrographs of the oxide scale formed, a) after 4h at 1200ºC in steam, alloy 106ZY-40h, b) after 4h at 1200ºC in steam, alloy 125YZ and c) after 4h at 1400ºC in air, alloy 106ZY-40h, d) after 4h at 1400ºC in steam, alloy 125YF. Scale bars for c) and d) are ten times larger than scale bars for a) and b). The white arrow highlights an area where the scale is locally protective

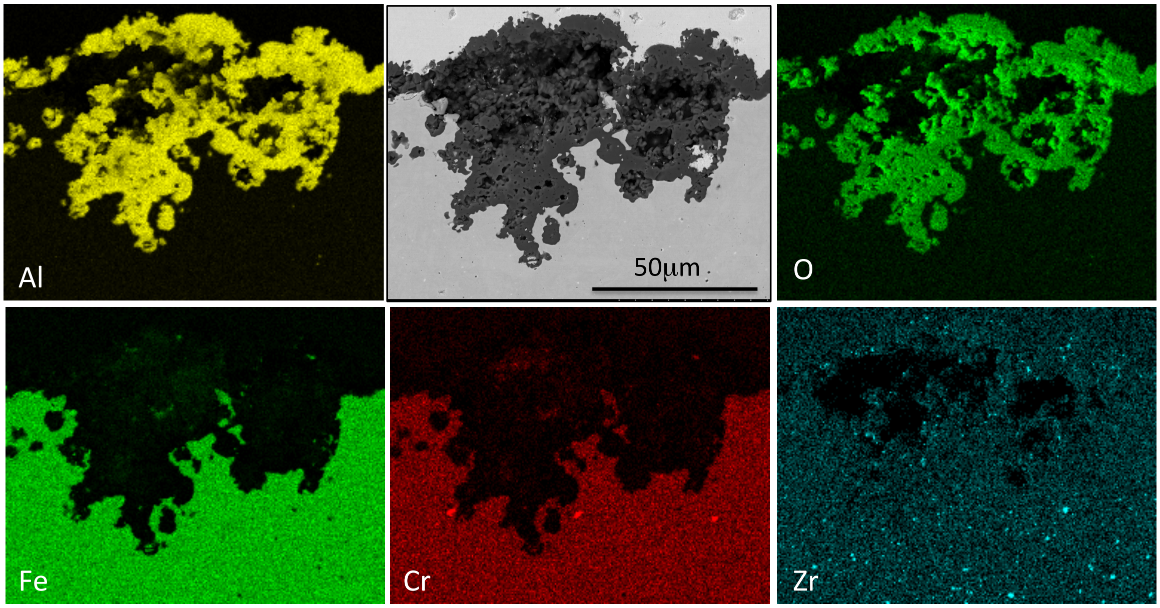

Figure 10: EDX mapping of the scale formed on alloy 106ZY-40h after 4h at 1400ºC in air

4. DISCUSSION AND FUTURE WORK

Our results show that the ODS FeCrAl fabrication parameters have a significant effect on the alloy microstructure and tensile properties. Ball milling for shorter times and extruding at higher temperatures offers ways to improve the alloy ductility and reduce the alloy strength, which will facilitate tube processing. On the contrary, small variations in Zr and Cr concentrations did not significantly impact the mechanical performance of the ODS FeCrAl alloys. Regarding the alloy impurity content, limiting the C content to less than 100ppm, as was achieved with the alloys ball milled 10h and 20h only, might play a role in the improved ductility of these alloys. However, variations of N content between 150ppm and 900pmm, and O content between 1100ppm and 2000ppm did not affect the alloy tensile properties. All the 2nd generation ODS alloys exhibited significantly better ductility than the 1st generation ODS alloys, with a plastic deformation of ~15-17% for the 2nd generation alloys in comparison with 5 to 10% for alloy 125YZ. It is however not clear if this is due to the addition of Zr (or Zr and Ti) directly in the gas atomized powder. The 12Cr-5.5Al-0.5Zr powder was, indeed, used to fabricate an alloy for the fusion program by extruding a 4 inch can through a rectangular die at 950ºC, to mimic the fabrication process of the 1st generation 125YZ alloy. The resulting alloy showed low ductility, which indicates that the better ductility of the 2nd generation alloys in comparison with the first gen ODS FeCrAl alloys is more likely due to the change in extrusion parameters. The tensile properties of these alloys are clearly dependent on the alloy grain structure, but further SEM and TEM characterization is needed to determine the role played by the various nano precipitates in the alloy tensile behavior.

ORNL is currently discussing the fabrication of ~500um thick tubes with an industrial partner, and over 4kg of ball milled 106ZY powder has been produced so far to fabricate master rods. Fabrication of these tubes will involve various fabrication steps, such as cold or warm working and high temperature heat treatments, that will affect the alloy microstructure and properties.[16,17] The impact of these fabrications steps on the microstructure and properties of the 2nd generation ODS FeCrAl alloys is being investigated.

5. CONCLUSION

A 2nd generation of ODS FeCrAl alloys fabricated by ball milling Fe-10-12Cr-6Al-Zr powder with Y_2O_3 powder showed plastic elongation at rupture over 15% at temperature ranging from 25 to 800ºC. Reducing the ball milling duration or increasing the extrusion temperature led to a decrease of the alloy strength but an increase in ductility. Variation of the Zr, Cr, O and N content did not affect significantly the alloy tensile properties. Future work will focus on the alloy processing to fabricate thin tubes.

6. ACKNOWLEDGMENTS

The authors would like to thank J. Turan, M. Howell, T Jordan, T. Lowe, C. Stevens, D. Harper and D. Hoelzer for their help with the experimental work. They want also to acknowledge M. Brady and B.A, Pint for reviewing the manuscript. This research was sponsored by the U.S. Department of Energy, FCRD Advanced Fuels Campaign Program.

7. REFERENCES

[1] S.J. Zinkle, K.A. Terrani, J.C. Gehin, L.J. Ott, L.L. Snead, "Accident tolerant fuels for LWRs: A perspective", Journal of Nuclear Materials, 448, 374-379 (2014).
[2] K. A. Terrani, S. J. Zinkle, L. L. Snead, "Advanced oxidation-resistant iron-based alloys for LWR fuel cladding", Journal of Nuclear Materials, 448, 420-435 (2014).
[3] T. Cheng, J. R. Keiser, M. P. Brady, K. A. Terrani and B. A. Pint, "Oxidation of fuel cladding candidate materials in steam environments at high temperature and pressure", Journal of Nuclear Materials, 427, 396-400 (2012).
[4] B. A. Pint, K. A. Unocic and K. A. Terrani, "The Effect of Steam on the High Temperature Oxidation Behavior of Alumina-Forming Alloys", Materials at High Temperatures, 32, 28-35 (2015).
[5] Y. Yamamoto, B.A. Pint, K.A. Terrani, K.G. Field, L.L. Snead, "Letter report documenting identifying billets and alloys fabricated for distribution to program" M3FT-13OR0202291, ORNL/LTR-2013/322, Oak Ridge National Laboratory (2013).
[6] Y. Yamamoto, B.A. Pint, K.A. Terrani, K.G. Field, Y. Yang, and L.L. Snead, "Development and property evaluation of nuclear grade wrought FeCrAl fuel cladding for light water reactors", Journal of Nuclear Materials, 467, 703-716 (2015).
[7] K. G. Field, X. Hu, K. C. Littrell, Y. Yamamoto, L. L. Snead, "Radiation tolerance of neutron-irradiated model FeCrAl alloys", Journal of Nuclear Materials, 465, 746-755 (2015).
[8] N.M. George, K.A. Terrani, J.J. Powers, "Neutronic analysis of candidate accident-tolerant iron alloy cladding concepts", ORNL report TM-2013/121 (2013).
[9] B. A. Pint, S. Dryepondt, K. A. Unocic and D. T. Hoelzer, "Development of ODS FeCrAl for Compatibility in Fusion and Fission Energy Applications", JOM 66 (2014) 2458.
[10] S. Dryepondt, K. A. Unocic, D. T. Hoelzer, B. A. Pint, "Advanced ODS FeCrAl Alloys For Accident-Tolerant Fuel Cladding", ORNL report, ORNL/TM-2014/380 (2015).
[11] K.A. Unocic, D. T. Hoelzer and B. A. Pint, "The Microstructure and environmental resistance of low Cr ODS FeCrAl," Materials at High Temperatures, 32, 123-132 (2015).
[12] K. A. Unocic, B. A. Pint, and D. T. Hoelzer, "Advanced TEM characterization of oxide nanoparticles in ODS Fe–12Cr–5Al alloys", Journal of Materials Science, 51, 9190-9206 (2016).
[13] P. Dou, A. Kimura, R. Kasada, T. Okuda, M. Inoue, S. Ukai, S. Ohnuki, T. Fujisawa, F. Abe, "TEM and HRTEM study of oxide particles in an Al-alloyed high-Cr oxide dispersion strengthened steel with Zr addition", Journal of nuclear materials, 444, 441-453 (2014).
[14] N.J. Cunningham,Y. Wu, A. Etienne, E.M. Haney, G.R. Odette, E. Stergar, D.T. Hoelzer, Y.D. Kim, B.D. Wirth and S.A. Maloy, "Effect of bulk oxygen on 14YWT nanostructured ferritic alloys", Journal of nuclear materials, 444, 35-38 (2014).

[15] P. Dou, A. Kimura, T. Okuda, M. Inoue, S. Ukai, S. Ohnuki, T. Fujisawa and F. Abe, "Effects of extrusion temperature on the nano-mesoscopic structure and mechanical properties of an Al-alloyed high-Cr ODS ferritic steel", Journal of Nuclear Materials, 417, 166-170 (2011).
[16] S. Ukai, M. Harada, H. Okada, M. Inoue, S. Nomura, S. Shikakura, T. Nishida, M. Fujiwara and K. Asabe, "Tube manufacturing and mechanical properties of oxide dispersion strengthened ferritic steel", Journal of nuclear materials, 204, 74-80 (1993)
[17] S. Ukai and M. Fujiwara, "Perspective of ODS alloys application in nuclear environments", Journal of Nuclear Materials, 307-311, 749-757 (20